Understanding the nature of "superhard graphite"

Supplementary Information

Salah Eddine Boulfelfel,[1,*] Artem R. Oganov,[1,2] and Stefano Leoni[3]

[1]*Stony Brook University, Department of Geosciences, NY 11794-2100, USA*

[2]*Department of Geology, Moscow State University, 119899 Moscow, Russia*

[3]*Technische Universität Dresden, Institut für Physikalische Chemie, 01062 Dresden, Germany*

[*]Electronic address: sboulfelfel@notes.cc.sunysb.edu

I. DFTB PARAMETERS FOR CARBON

DFTB total energy calculations were performed using DFTB+ code, version 1.1 (Aradi B, Hourahine B, Frauenheim Th (2007) DFTB+, a Sparse Matrix-Based Implementation of the DFTB Method *J Phys Chem A* 111:5678-5684), and the dispersion correction was included to account for van der Waals interactions between graphitic layers (Zhechkov L, Heine T, Patchkovskii S, Seifert G, Duarte HA (2005) An efficient *a Posteriori* treatment for dispersion interaction in density-functional-based tight binding *J Chem Theory Comput* 1:841-847).

DFT total energy calculations were performed using QUANTUM ESPRESSO package, version 4.3.2 (Giannozzi P *et al.* (2009) QUANTUM ESPRESSO: a modular and open-source software project for quantum simulations of materials *J Phys: Condens Matter* 21:395502-395521), and the dispersion correction was included to account for van der Waals interactions between graphitic layers (Barone V *et al.* (2009) Role and effective treatment of dispersive forces in materials: Polyethylene and graphite crystals as test cases *J Comp Chem* 30:934-939 and Grimme S (2006) Semiempirical GGA-type density functional constructed with a long-range dispersion correction *J Comp Chem* 27:1787-1799).

For both DFT and DFTB, a full variable-cell relaxation was performed for each structure.

The dispersion correction stabilized hexagonal graphite by 87 meV/atom (Fig. 1) and 62 meV/atom (Fig. 2) using DFTB and DFT (GGA), respectively.

TABLE I: Comparison between DFT and DFTB total energies of different structures of carbon investigated in TPS simulations.

	DFT-LDA	DFT-GGA	DFTB
graphite	-155.682 (0.000)	-155.161 (0.000)	-46.985 (0.000)
diamond (cubic)	-155.535 (0.147)	-154.910 (0.251)	-46.796 (0.189)
W-carbon	-155.356 (0.326)	-154.755 (0.406)	-46.607 (0.378)
M-carbon	-155.347 (0.335)	-154.747 (0.414)	-46.602 (0.383)
bct C_4	-155.304 (0.378)	-154.712 (0.449)	-46.574 (0.411)

Energies are given in eV/atom.

Dispersion correction used for graphite in both DFT and DFTB.

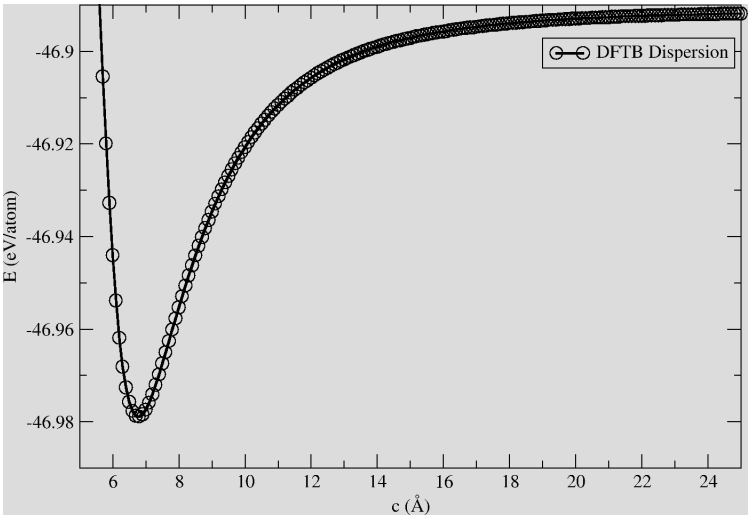

FIG. 1: DFTB total energy variation of graphite in function of interlayer separation. Dispersion correction was included to account for van der Waals interactions. For each step, the structure was relaxed within *ab* plane while keeping *c* unchanged.

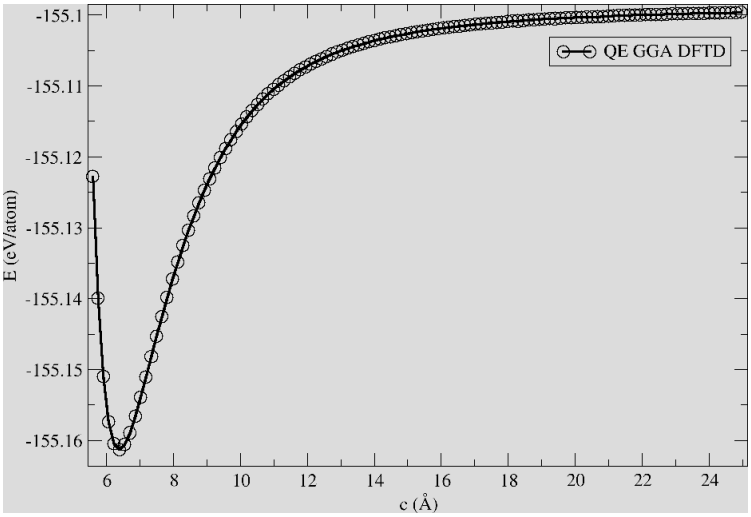

FIG. 2: DFT total energy variation of graphite in function of interlayer separation. Dispersion correction was included to account for van der Waals interactions. For each step, the structure was relaxed within *ab* plane while keeping *c* unchanged.

II. ORIENTATION RELATIONS BETWEEN GRAPHITE AND *o*C16 STRUCTURES

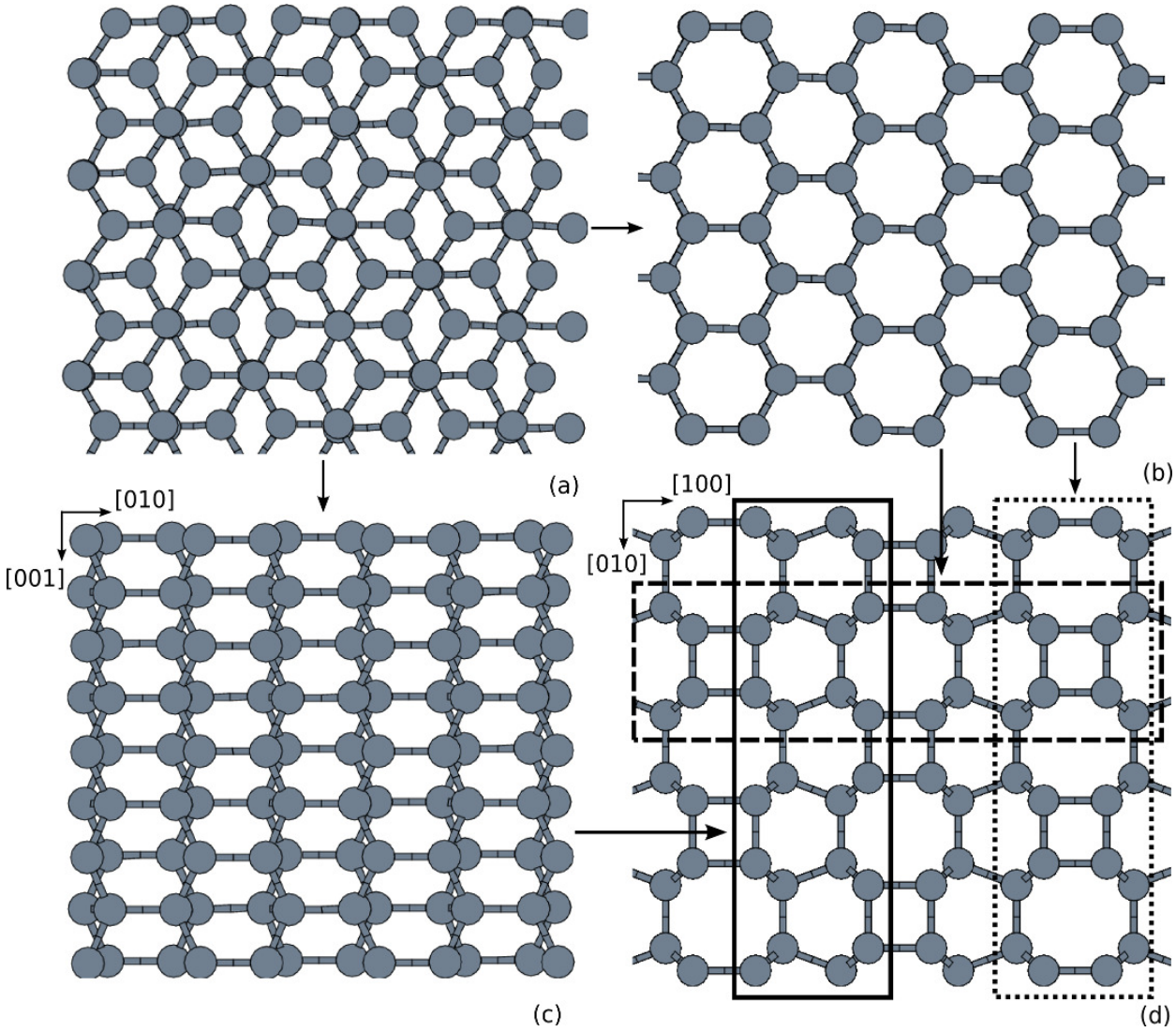

FIG. 3: Different sliding mechanisms for the (a) graphite to (d) *o*C16 transformation. Three different slabs of *o*C16 are highlighted with plain, dotted, and dashed frames and the satcking is compared to graphite. Large atomic displacements in terms of graphitic layer sliding in order to initiate nucleation of *o*C16 strcuture.